

## RESEARCH ARTICLE

### GW correlation effects on plutonium quasiparticle energies: changes in crystal-field splitting

A. N. Chantis<sup>a\*</sup>; <sup>a</sup>R. C. Albers; <sup>b</sup>A. Svane; <sup>b</sup>N. E. Christensen

<sup>a</sup>*Theoretical Division, Los Alamos National Laboratory, Los Alamos, New Mexico, 87545, USA;* <sup>b</sup>*Department of Physics and Astronomy, University of Aarhus, DK-8000 Aarhus C, Denmark*

()

We present results for the electronic structure of plutonium by using a recently developed quasiparticle self-consistent *GW* method (QSGW). We consider a paramagnetic solution without spin-orbit interaction as a function of volume for the face-centered cubic (fcc) unit cell. We span unit-cell volumes ranging from 10% greater than the equilibrium volume of the  $\delta$  phase to 90 % of the equivalent for the  $\alpha$  phase of Pu. The self-consistent *GW* quasiparticle energies are compared to those obtained within the Local Density Approximation (LDA). The goal of the calculations is to understand systematic trends in the effects of electronic correlations on the quasiparticle energy bands of Pu as a function of the localization of the *f* orbitals. We show that correlation effects narrow the *f* bands in two significantly different ways. Besides the expected narrowing of individual *f* bands (flatter dispersion), we find that an even more significant effect on the *f* bands is a decrease in the crystal-field splitting of the different bands.

**Keywords:** Plutonium, electron correlations, GW approximation, first-principles electronic structure

#### 1. Introduction

Much of our modern understanding of electronic correlations in narrow-band systems has derived from many-body treatments of model-Hamiltonian systems such as the Hubbard model and the Anderson model. For example, with respect to plutonium in particular, dynamical mean-field theory (DMFT) approaches have been very useful in elucidating the physics of the very strong correlations in this material (see, for example, Refs. [1] and [2] and references therein). Nonetheless, these calculations are not first principles, and most of the physics comes from the model part of the Hamiltonian rather than the band-structure part of the calculations. Thus, it is still important to better understand the multi-orbital and hybridization effects in more realistic electronic-structure approaches that are less model dependent. The *GW* method is our best modern tool to examine these effects, because it includes correlation effects beyond that of conventional local-density approximation (LDA) band-structure techniques and yet is still first-principles.

In this paper we study correlation effects of fcc Pu as a function of volume. Our goal is not to specifically elucidate the correlation physics of Pu itself, since the *GW* approach is a low-order approximation and cannot treat the very strong correlations

---

\*Corresponding author. Email: [achantis@lanl.gov](mailto:achantis@lanl.gov)

of the  $\delta$  phase of Pu. Rather, we wish to use the volume dependence to tune the material from high atomic density (high pressure), where correlations can be greatly reduced due to the large hybridization between the Pu  $f$  orbitals, to low atomic densities (where the pressure would actually be in tension), where the correlations effects are very strong. By following this procedure, we can understand how correlations modify the properties of a material *within the GW approximation*. When the correlations become strong, it is certainly the case that higher-order approximations like DMFT are necessary to accurately describe the material. Nonetheless, since GW is probably the correct starting point for such types of more sophisticated approaches, it is still useful to understand what happens to the electronic-structure of the material within the GW approximation as a function of the strength of the correlation effects, and, in particular, their effects on shifts in quasi-particle energies, which is what GW is best at representing.

In order to focus more specifically on the effects of correlations, we ignore one significant aspect of the electronic structure, viz., the spin-orbit coupling, even though this is important for a detailed comparison with experiment. Spin-orbit coupling mainly shifts  $f$  states around in energy, but at the same time add to the complexity of the individual  $f$  bands, hence tending to hide some of the correlation physics in a bewildering array of bands. Spin-orbit effects can easily be added in when a more accurate comparison with experiment is desired (as was done for an earlier paper on less correlated  $\alpha$  uranium [3]).

For the same reasons we also ignore well-known large changes in crystal structure of Pu metal with volume, and present calculations only for the simple fcc crystal structure as a function of volume. We study a range of Pu atomic volumes extending from well below that pertinent to the ground state  $\alpha$  phase to well above that of the high-temperature  $\delta$  phase. The actual crystal structure of  $\alpha$ Pu is a complicated monoclinic structure with 16 atoms per unit cell, while  $\delta$ Pu has the fcc structure. Since  $\delta$ Pu is well known to be a strongly correlated-electron metal while  $\alpha$ Pu appears to be reasonably well treated by conventional band-structure methods, we believe that our range of volumes corresponds to tuning the correlation effects between weak to moderate (small volumes) to strongly correlated (large volumes).

In the calculations to be presented in the following we mainly focus on changes in the effective bandwidth of the  $f$  states in Pu. We will show that crystal-field effects are actually a more important factor in determining this bandwidth than the expected change in dispersion (flattening of the bands).

## 2. Method

The *GW* approximation can be viewed as the first term in the expansion of the non-local energy-dependent self-energy  $\Sigma(\mathbf{r}, \mathbf{r}', \omega)$  in the screened Coulomb interaction  $W$ . From a more physical point of view it can be interpreted as a dynamically screened Hartree-Fock approximation plus a Coulomb-hole contribution [4]. It is also a prescription for mapping the non-interacting Green function onto the dressed Green's function:  $G^0 \rightarrow G$ . This prescription can be described as follows. From the Hamiltonian

$$H_0 = -\nabla^2 + V_{\text{eff}}(\mathbf{r}, \mathbf{r}') \quad (1)$$

(we use atomic Rydberg units:  $\hbar = 2m = e^2/2 = 1$ , where  $m$  and  $e$  are the mass and charge of the electron)  $G^0 = (\omega - H_0)^{-1}$  may be constructed. Often  $G^0$  is calculated from the LDA eigenvalues and eigenfunctions; however, there is no formal restriction for how to choose the initial starting point  $G^0$ . Then, using

the Random Phase Approximation (RPA) [4], we can construct the polarization function  $D$  and screened Coulomb interaction  $W$  as

$$D = -iG^0 \times G^0 \quad (2)$$

and

$$W = u \times \frac{1}{1 - uD}, \quad (3)$$

where  $u$  is the bare Coulomb interaction. The new Green's function is defined as

$$G = \frac{1}{\omega - (-\nabla^2 + V^{\text{ext}} + V^{\text{H}} + \Sigma)}, \quad (4)$$

where  $V^{\text{ext}}$  is the potential due to ions (Madelung) and  $V^{\text{H}}$  is the Hartree potential

$$V^{\text{H}}(\mathbf{r}) = 2 \int d\mathbf{r}' \frac{n(\mathbf{r}')}{|\mathbf{r} - \mathbf{r}'|}. \quad (5)$$

The single-particle density  $n(\mathbf{r})$  is calculated as  $n(\mathbf{r}) \sim \int_{-\infty}^{\infty} d\omega G^0(\mathbf{r}, \mathbf{r}, \omega) e^{i\omega\delta}$ .

In addition to this mapping of  $G^0 \rightarrow G$ , one can also generate an excellent effective potential from  $G$  that makes it possible to approximately do the inverse mapping of  $G \rightarrow G^0$  [5]. The QSGW is a method to specify this (nearly) optimal mapping of  $G \rightarrow G^0$ , so that  $G^0 \rightarrow G \rightarrow G^0 \rightarrow \dots$  can be iterated to self-consistency [5, 6]. At self-consistency the quasiparticle energies of  $G^0$  coincide with those of  $G$ . Thus QSGW is a self-consistent perturbation theory, where the self-consistency condition is constructed to minimize the size of the perturbation. The QSGW method is parameter-free, and independent of basis set as well as the LDA starting point [5–7]. We have previously shown that QSGW reliably describes a wide range of *spd* [5, 8–11], and rare-earth [12] systems. We have also applied the method to calculate the electronic structure of  $\alpha$ -uranium [3].

Our version of the QSGW method is based upon the Full Potential Linear Muffin Tin Orbital (FP-LMTO) method [13], which makes no approximation for the shape of the crystal potential. The smoothed LMTO basis [7] includes orbitals with  $l \leq l_{\text{max}} = 6$ ; both  $7p$  and  $6p$  as well as both  $5f$  and  $6f$  are included in the basis. The  $6f$  orbitals are added as a local orbital [7], which is confined to the augmentation sphere and has no envelope function. The  $7p$  orbital is added as a kind of extended ‘local orbital,’ the ‘head’ of which is evaluated at an energy far above Fermi level [7] and instead of making the orbital vanish at the augmentation radius a smooth Hankel ‘tail’ is attached to the orbital. The  $7p$  and  $6f$  orbitals are necessary to obtain an accurate description of highlying bands, which are important for the accuracy of the polarization function in Eq. (2). For our calculations we use the fcc Pu lattice with the following lattice constants  $a=4.11 \text{ \AA}$  (which corresponds to 90% of the  $\alpha$ -Pu equilibrium volume),  $4.26 \text{ \AA}$  (at the  $\alpha$ -Pu equilibrium volume),  $4.64 \text{ \AA}$  (at the  $\delta$ -Pu equilibrium volume) and  $4.79 \text{ \AA}$  (at 110% of the  $\delta$ -Pu equilibrium volume).

### 3. Results

In Fig.1 we compare the QSGW one-particle electronic structure of  $\delta$ -Pu with the LDA band-structure results. The spin-orbit interaction is not included in this

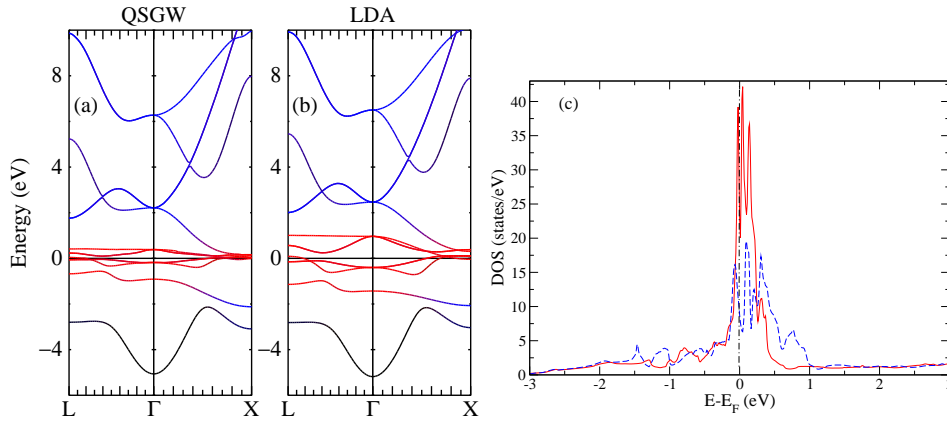


Figure 1. (color online). (a) The QSGW energy bands (or quasi-particle energies) for  $\delta$ -Pu along two symmetry directions (left panel), compared to (b) the LDA energy bands (right panel); the Mulliken weights of the  $f$  orbitals are presented in red (dark gray), for  $s$  orbitals in black and for  $d$  orbitals in blue (light gray). (c) Comparison of the total density of states (DOS) for QSGW, red (dark gray) solid line, and LDA, blue (light gray) dashed line. The Fermi energy is set at zero.

calculation. The Mulliken weights of the  $f$  orbitals are presented in red (dark gray), of the  $s$  orbitals in black and of the  $d$  orbitals in blue (light gray). In both cases, the narrow bands located between -2 and 2 eV are predominantly due to seven  $5f$  orbitals. At the  $\Gamma$  point they are split by the cubic crystal field into one nondegenerate and two three-fold degenerate states. This degeneracy is reduced at general  $k$ -points in the Brillouin zone. The lowest dispersive band centered around -4 eV has primarily  $s$  character and the unoccupied bands above 2 eV are mainly due to  $d$  orbitals. At the  $\Gamma$  point the five  $d$  states are split by the cubic crystal field into one two-fold degenerate and one three-fold degenerate state. The  $sdf$  hybridization along the symmetry directions presented in Fig. 1 is generally very weak except for near the  $X$  point along the  $\Gamma - X$  direction, where there is very strong  $sd$  and  $df$  hybridization for some of the  $d$  and  $f$  branches. The degree of the hybridization is very similar in both the LDA and QSGW calculations, as is the center of all of the bands. The largest visible change is a significant narrowing of the  $5f$ -band complex. This effect has two components: first, the crystal-field splitting of the  $f$  bands is significantly reduced in QSGW, second, the bandwidth of each individual  $f$  branch (band) is also reduced in QSGW. The total effect appears as an overall narrowing of the total density of states (DOS) around the Fermi level (see Fig. 1(c)). In addition, since the area under the curve is proportional to the number of  $5f$  states, which remains constant, the amplitude of the quasiparticle peaks are also higher in QSGW. For example, the total DOS at the Fermi level in QSGW is 23 states/eV while in LDA it is 9 states/eV.

The partial DOS is presented in Fig. 2. In both calculations the partial- $5f$  DOS is concentrated in a narrow energy interval around  $E_F$ . The partial- $s$  DOS is mainly located in the occupied energy spectrum between -5 eV and  $E_F$  and the  $d$  bands are spread in a wide energy interval in both the unoccupied and occupied part of the spectrum with a few pronounced peaks at various energies. Overall, the QSGW and LDA  $s$  and  $d$  peaks are located at the same energies, with the exception of the narrow peaks around  $E_F$ , in which case the QSGW are visibly shifted closer to  $E_F$ . In this region these bands can be highly hybridized with the  $f$  states, and thus these shifts reflect the band narrowing of the  $f$  states. The bottom of the  $s$  and  $d$  bands relative to the position of  $f$  band is approximately at the same energy location in QSGW and LDA. The  $f$  occupation changes in QSGW from its LDA value of 5.06 to 4.85 states. A similar reduction was observed in our calculations for  $\alpha$ -uranium [3].

In Fig. 3 we present side by side the band structures for two different fcc volumes. On the left side is the band structure and partial  $s$  and  $d$  DOS for the  $\alpha$  volume (weakly correlated) and on the right side is the band structure and partial  $s$  and  $d$  DOS for the  $\delta$  volume (strongly correlated). In all cases, the red solid lines represent the QSGW results and the dashed-blue lines show the LDA results. Two major effects are seen in this plot: (1) the  $f$  bands narrow considerably with expanded volume, and (2) there is a similar effect on the  $d$  bands (notice the downward shift

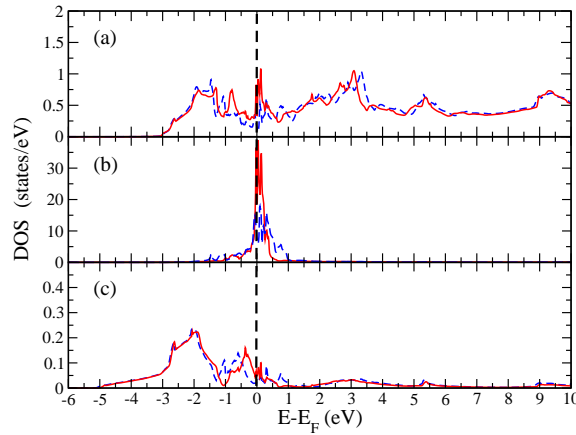


Figure 2. (color online). Comparison of QSGW, red (dark gray) solid line, and LDA, blue (light gray) dashed line, partial DOS for (a) the  $d$  orbitals, (b) the  $f$  orbitals, and (c) the  $s$  orbitals.

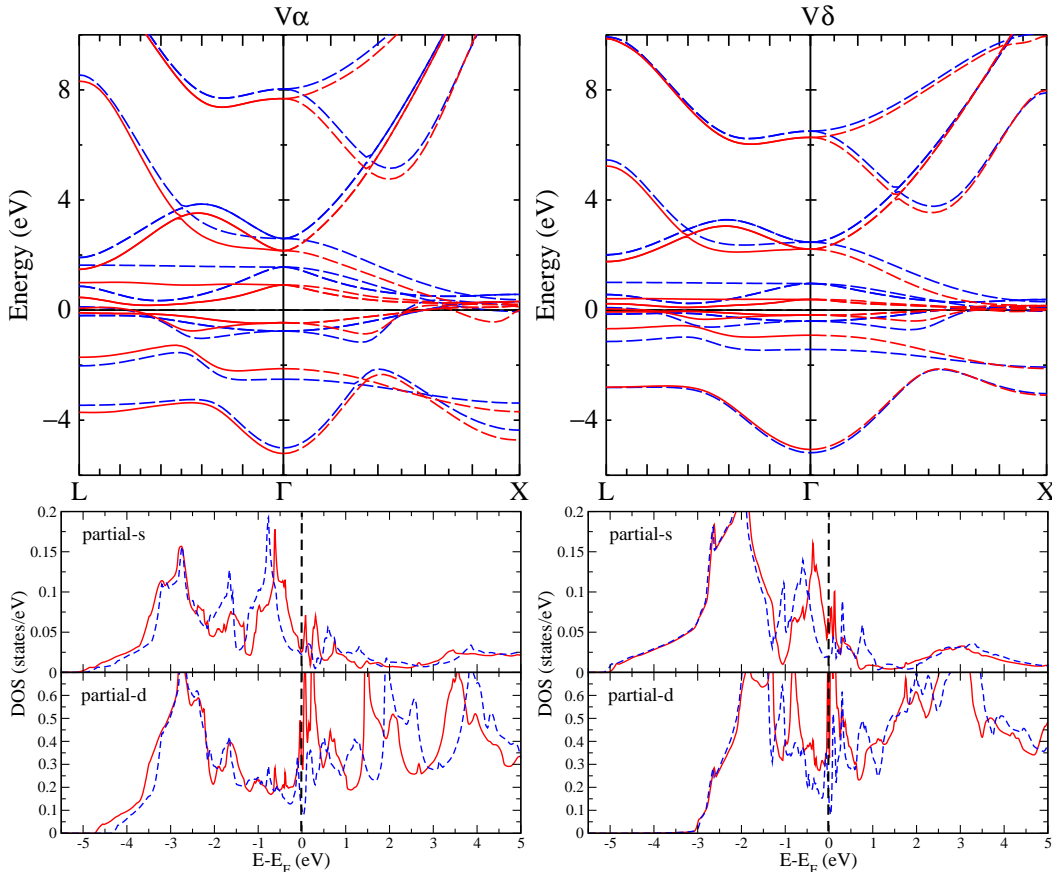


Figure 3. (color online). Comparison of the QSGW, red (dark gray) solid line, and LDA, blue (light gray) dashed line, band structure. On the left side are the energy bands for the more weakly correlated case for  $a=4.26 \text{ \AA}$  (equivalent to the density of atoms for the  $\alpha$ -Pu equilibrium volume), and on the right side the more strongly correlated case of  $a=4.64 \text{ \AA}$  (the  $\delta$ -Pu equilibrium volume).

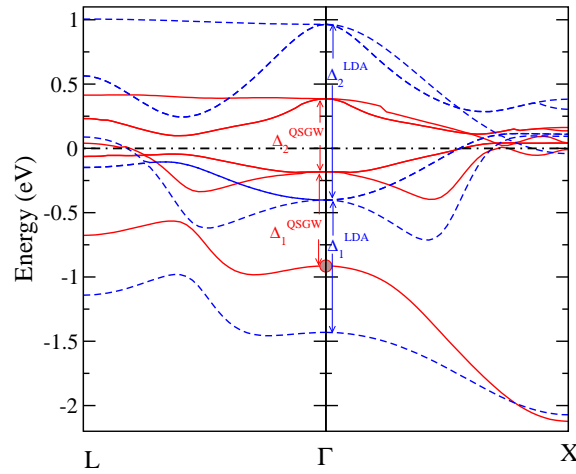


Figure 4. (color online). Comparison of QSGW, red (dark gray) solid line, and LDA, blue (light gray) dashed line, energy bands along two symmetry directions. The magnitude of crystal field splittings  $\Delta_1$ ,  $\Delta_2$  are 1.02, 1.37 eV in LDA and 0.73, 0.57 eV in QSGW.  $\Delta_2$  is reduced significantly in QSGW calculation. For the  $5f$  state at the  $\Gamma$  point, marked with a large dot, in Fig. 5 we present the energy dependence of the self-energy and calculated spectral function  $A(\omega)$

of the bands at the highest energy as one goes from the  $\alpha$  to the  $\delta$  volume).

To examine band narrowing effects in more detail, in Fig. 4 we expand the view of the  $5f$  bands. Also, in Fig. 5 we show the self-energy and spectral function for one of the QSGW  $5f$  states. Despite of the complicated energy dependence of the real and imaginary parts it appears that the state is described perfectly well by Landau's Fermi liquid theory. The imaginary part of the self-energy goes through zero at  $E_F$  and the spectral function has a *single* well defined peak centered at the QSGW eigenvalue. There are no other pronounced features in the energy dependence of the spectral function. This is representative of all  $5f$  states. So the  $5f$  states within the QSGW theory are well defined quasiparticles with very large lifetime around  $E_F$ ; the QSGW eigenvalues coincide with the quasiparticle energy. Therefore, our discussion is focused on the effects of electron correlations on the QSGW eigenvalues. At the  $\Gamma$  point the  $f$  orbitals are split by the cubic crystal field into a nondegenerate state  $A_2$  and two three fold degenerate states  $T_1$  and  $T_2$ . The splitting,  $\Delta_1$ , between the nondegenerate state and the lowest of the three-fold degenerate states is 1.02 eV in LDA and 0.73 eV in QSGW. The splitting,  $\Delta_2$ , between the two three-fold degenerate states is equal to 1.37 eV in LDA but only 0.57 eV in QSGW. This significant reduction of the crystal field splitting in QSGW is the major part of the band narrowing observed in the DOS

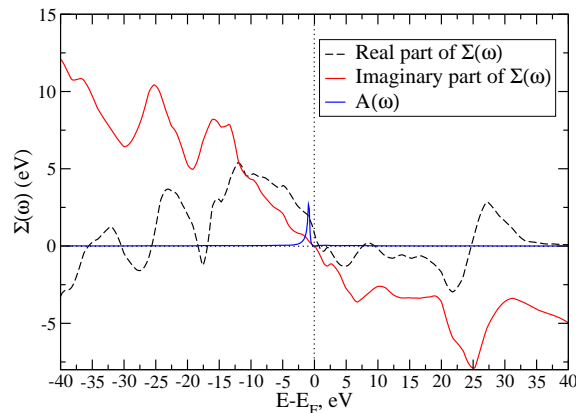


Figure 5. The energy dependence of the real and imaginary part of self-energy together with the spectral function for the quasiparticle at  $\mathbf{k} = (0, 0, 0)$  and  $E_0 = -0.917$  eV.

Table 1. The band width of Pu 5*f* bands along  $L - \Gamma$  and  $\Gamma - X$  symmetry directions. The band width is defined as the difference between the maximum and the minimum energy of a particular band along the direction. The width is given in eV

	$L - \Gamma$	$\Gamma - X$
$A_2$ LDA	0.48	0.64
$A_2$ QSGW	0.43	1.21
$T_1$ LDA	0.71	0.83
$T_1$ QSGW	0.38	0.44
$T_2$ LDA	0.77	1.02
$T_2$ QSGW	0.32	0.45

in Fig. 1. Another important aspect is the reduction of the width of each individual *f* band. In Table 1 we present the values of the band width of Pu 5*f* bands along  $L - \Gamma$  and  $\Gamma - X$  symmetry directions. The band width is defined as the difference between the maximum and the minimum energy of a particular band along the direction. In all cases the band width is reduced significantly in QSGW. The  $A_2$  band along  $\Gamma - X$  is a striking exception from this rule. As we show in Fig. 6 this band strongly hybridizes with the *d* states. At the  $\Gamma$  point it is 100% *f* but at the  $X$  point it is predominately *d*. All the other bands shown in Fig. 4 remain 80 to 100% *f* throughout the symmetry directions shown in the figure. This explains the anomalous change in the width of this band for this particular direction. From Fig. 3 it is evident that, while in QSGW the width of the *f* bands are significantly reduced, the width of *d* bands are practically the same as for LDA. The  $A_2$  band at the  $\Gamma$  point has mainly *f* character and therefore moves upward from its LDA position due to the significant reduction of the *f* crystal field in QSGW, but at the  $X$  point mainly has *d* character and therefore remains approximately at its LDA position (only slightly lower due to the slight downward shift of the center of *d* band in QSGW). The cumulative effect is that in QSGW this band is stretched.

In Tables 2 and 3 we show the values for the crystal field splitting of 5*f* bands and *f* band widths along  $L - \Gamma$  for several volumes of the unit cell. The band width and crystal field splitting of all bands is reduced as we move from the lower to higher volume case. This is a result of the reduction of the *f* band relative extend in the crystal. It is also seen that the QSGW crystal field splittings and band widths for *f* orbitals are always smaller than in LDA. We have also considered the band width

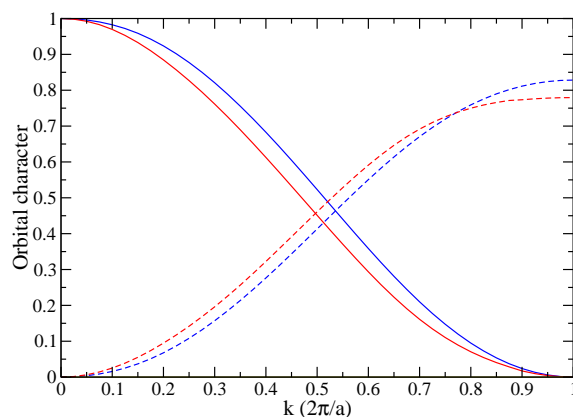


Figure 6. (color online). QSGW, red (dark gray) solid line, and LDA, blue (light gray) solid line *f*-orbital weight of the  $A_2$  band along  $\Gamma - X$  direction. Also shown is the QSGW, red (dark gray) dashed line, and LDA, blue (light gray) dashed line *d*-orbital weight of the  $A_2$  band along the same direction

Table 2. The crystal field splitting  $\Delta_1$  and  $\Delta_2$  of Pu 5f states at the  $\Gamma$  point. The QSGW values for the splitting are significantly smaller than those of LDA calculation. The energy splitting is given in eV

	0.9 $V_\alpha$	$V_\alpha$	$V_\delta$	1.1 $V_\delta$
$\Delta_1^{LDA}$	2.14	1.75	1.02	0.84
$\Delta_1^{QSGW}$	2.09	1.67	0.73	0.51
$\Delta_2^{LDA}$	2.86	2.33	1.37	1.11
$\Delta_2^{QSGW}$	1.96	1.36	0.57	0.41

Table 3. The band width of Pu 5f bands along  $L - \Gamma$  symmetry directions for different volumes of the unit cell. The band width is defined as the difference between the maximum and the minimum energy of a particular band along the direction. We also provide the full width at half maximum (FWHM) of the broadened  $f$ -partial DOS shown in Fig. 7. The width is given in eV

	0.9 $V_\alpha$	$V_\alpha$	$V_\delta$	1.1 $V_\delta$
$A_2$ LDA	1.42	1.0	0.48	0.37
$A_2$ QSGW	1.23	0.94	0.43	0.30
$T_1$ LDA	1.38	1.15	0.71	0.6
$T_1$ QSGW	1.17	0.86	0.38	0.28
$T_2$ LDA	1.62	1.29	0.77	0.63
$T_2$ QSGW	1.30	0.84	0.32	0.23
FWHM LDA	1.28	1.09	0.78	0.72
FWHM QSGW	0.79	0.63	0.39	0.34

of the entire 5f band complex. To do this we have applied a Gaussian broadening on the partial- $f$  DOS (Fig. 7). In this case the 5f band complex appears like a single large peak. We can define the width of this band as the full width at half maximum (FWHM) of the peak. This is also presented in Table 3. It is evident that in both calculations the width is reduced as the volume increases. The rate of reduction is the same in both calculations. But the QSGW FWHM is always significantly smaller than the LDA. Therefore, we conclude that in QSGW the  $f$  orbitals contract due to the more accurate treatment of correlations. On the other hand, the  $s$  and  $d$  bands are very itinerant and are therefore already described accurately at the level of the LDA treatment of correlations.

#### 4. Conclusions

In conclusion, we have applied QSGW theory to  $\delta$  plutonium as a function of volume in order to systematically understand the effects of electronic correlation on the band narrowing of the  $f$  bands. Unlike conventional model-Hamiltonian treatments of strongly correlated systems our approach is first principles and independent of any choice of model parameters, and hence provides a unique opportunity to examine the effect of electron correlations on the quasiparticle band structure as a function of  $f$ -orbital localization. In this way we have demonstrated that QSGW and LDA prediction for the  $s$  and  $d$  electron subsystems are quite similar. This is because these electrons are very itinerant and therefore their description lies within the validity of LDA. However, the QSGW 5f bands are much narrower than their LDA counterpart. We believe that our results for the first time show significant details of the band narrowing due to electron correlations that have not been previously studied. In particular, the QSGW calculations show that the



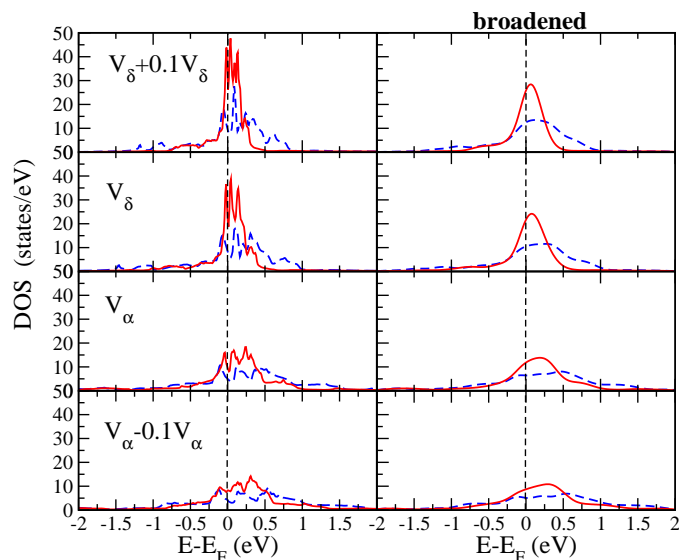


Figure 7. (color online). The QSGW and LDA  $f$ -partial DOS for four different volumes. The panels on the right side show the corresponding DOS on the left panel broadened with a Gauss function.

major contribution to band narrowing is actually the reduction of the crystal-field splitting of  $5f$  states as compared to effects from a reduction in dispersion (flattening of the individual bands). This is a significant change in the character of the  $5f$  states and suggests the importance of using GW approaches as input to more sophisticated correlation approaches such as dynamical mean-field theories (DMFT).

## 5. Acknowledgments

This work was carried out under the auspices of the National Nuclear Security Administration of the U.S. Department of Energy at Los Alamos National Laboratory under Contract No. DE-AC52-06NA25396. A.N.C would like to thank Mark van Schilfgaarde and Takao Kotani for informative discussions.

## References

- [1] C. A. Marianetti, K. Haule, G. Kotliar, and M. J. Fluss, Phys. Rev. Lett. 101 (2008) p. 056403
- [2] J. H. Shim, K. Haule, S. Savrasov, and G. Kotliar, Phys. Rev. Lett. 101 (2008) p. 126403
- [3] A. N. Chantis, R. C. Albers, M. D. Jones, M. van Schilfgaarde, and T. Kotani, Phys. Rev. B 78 (2008) p. 081101
- [4] L. Hedin, J. Phys.: Condens. Matter 11 (1999) p. R489
- [5] M. van Schilfgaarde, T. Kotani, and S. Faleev, Phys. Rev. Lett. 96 (2006) p. 226402
- [6] T. Kotani, M. van Schilfgaarde, and S. V. Faleev, Phys. Rev. B 76 (2007) p. 165106
- [7] M. van Schilfgaarde, T. Kotani, and S. V. Faleev, Phys. Rev. B 74 (2006) p. 245125
- [8] S. V. Faleev, M. van Schilfgaarde, and T. Kotani, Phys. Rev. Lett. 93 (2004) p. 126406
- [9] T. Kotani, M. van Schilfgaarde, S. V. Faleev and A. N. Chantis, J. Phys.: Condens. Matter (2007) p. 365236
- [10] A. N. Chantis, M. Cardona, N. E. Christensen, D. L. Smith, M. van Schilfgaarde, T. Kotani, A. Svane, and R. C. Albers, Phys. Rev. B 78 (2008) p. 075208
- [11] A. N. Chantis, M. van Schilfgaarde, and T. Kotani, Phys. Rev. Lett. 96 (2006) p. 086405
- [12] A. N. Chantis, M. van Schilfgaarde, and T. Kotani, Phys. Rev. B 76 (2007) p. 165126
- [13] M. Methfessel, M. van Schilfgaarde and R. A. Casali, in *Electronic Structure and Physical Properties of Solids: The Uses of the LMTO Method*, edited by H. Dreyse, Lecture Notes in Physics Vol. 535 (Springer-Verlag, Berlin, 2000)